

# Polymer Chemistry

Accepted Manuscript



This is an *Accepted Manuscript*, which has been through the Royal Society of Chemistry peer review process and has been accepted for publication.

*Accepted Manuscripts* are published online shortly after acceptance, before technical editing, formatting and proof reading. Using this free service, authors can make their results available to the community, in citable form, before we publish the edited article. We will replace this *Accepted Manuscript* with the edited and formatted *Advance Article* as soon as it is available.

You can find more information about *Accepted Manuscripts* in the [Information for Authors](#).

Please note that technical editing may introduce minor changes to the text and/or graphics, which may alter content. The journal's standard [Terms & Conditions](#) and the [Ethical guidelines](#) still apply. In no event shall the Royal Society of Chemistry be held responsible for any errors or omissions in this *Accepted Manuscript* or any consequences arising from the use of any information it contains.

## Synthesis of multicompartment nanoparticles of triblock terpolymer by seeded RAFT polymerization

Xin He, Yaqing Qu, Chengqiang Gao and Wangqing Zhang\*

Received 00th January 20xx,  
Accepted 00th January 20xx

DOI: 10.1039/x0xx00000x

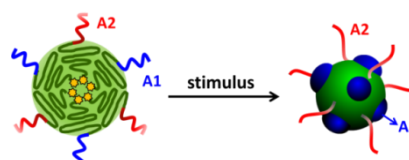
www.rsc.org/

**Abstract:** Seeded RAFT polymerization is proposed to prepare multicompartment nanoparticles of the poly(*N,N*-dimethylacrylamide)-*b*-polystyrene-*b*-poly(4-vinylpyridine) (PDMA-*b*-PS-*b*-P4VP) triblock terpolymer, which contain a polystyrene (PS) core, discrete poly(4-vinylpyridine) (P4VP) microphases on the PS core, and a solvated poly(*N,N*-dimethylacrylamide) (PDMA) corona. Following this seeded RAFT polymerization, the seed nanoparticles of poly(*N,N*-dimethylacrylamide)-*b*-polystyrene are initially prepared through dispersion RAFT polymerization, and then the P4VP block is introduced onto the seed nanoparticles by seeded RAFT polymerization to prepare the corona-core nanoparticles of PDMA-*b*-PS-*b*-P4VP containing a PS core and a mixed corona of P4VP and PDMA. When the corona-core nanoparticles of PDMA-*b*-PS-*b*-P4VP are dispersed in water, the P4VP chains, which are segregated by the neighboring PDMA chains, deposit onto the PS core to form the discrete P4VP microphases on the PS core, and they convert into multicompartment nanoparticles. It is found that the size of the P4VP microphases on the PS core increases with the polymerization degree of the P4VP block. This seeded RAFT polymerization is believed to be a valid method to prepare block copolymer multicompartment nanoparticles.

### 1 Introduction

Multicompartment block copolymer nanoparticles (MCBNs) containing a solvophilic corona and a solvophobic microphase-separated core have gained considerable attention.<sup>1–3</sup> The special structure of MCBNs affords their potential application in simultaneously entrapping or releasing different hydrophobic ingredients.<sup>3</sup> Generally, there are two strategies proposed to prepare MCBNs. The most straightforward method is the self-assembly of linear ABC block terpolymers, ABC miktoarm star terpolymers, and multiblock copolymers such as ABCA and ABCBA in the block-selective solvent for the A block, in which A represents the solvophilic block and B and C represent two incompatible solvophobic blocks throughout this article.<sup>4–19</sup> The second strategy to prepare MCMs is through the co-micellization or blending of two or more different block copolymers, such as AB with AC diblock copolymer or ABC block terpolymers or ABC miktoarm star terpolymers with AB diblock copolymer in a suitable block-selective solvent.<sup>20–33</sup> Recently, it is found that the core-corona block copolymer nanoparticles containing a mixing corona of two different blocks, e.g. the blue A1 and the red A2, can convert into MCBNs by depositing one corona-forming block

onto the core as shown in Scheme 1, if the deposited corona-forming block of A1 is incompatible with the green core-forming block.<sup>34–37</sup> The preparation of MCBNs is partly ascribed to the blue A1 block being segregated by the red neighboring A2 block when the A1 block chains deposit onto the core,<sup>38</sup> which makes the A1 chains to form discrete or separated microphases on the core of the corona-core nanoparticles to form MCBNs.



**Scheme 1.** The schematic synthesis of MCBNs from the block copolymer corona-core nanoparticles containing a mixing corona of two different blocks.

Seeded RAFT polymerization based on the pre-prepared AB diblock copolymer nano-objects has been demonstrated to be a valid method to prepare ABC or ABA triblock copolymer nano-objects.<sup>39–43</sup> Following this seeded RAFT polymerization, a new block is introduced into the pre-prepared AB diblock copolymer nano-objects just as similarly as those in the graft-through strategy to afford triblock copolymer nano-objects.<sup>44</sup> Recently, we have prepared ABA triblock copolymer core-corona particles following this seeded RAFT polymerization in the presence of the AB diblock copolymer nanoparticles.<sup>42,43</sup> It is found that the hydrodynamic diameter ( $D_h$ ) of the ABA

<sup>a</sup> Key Laboratory of Functional Polymer Materials of the Ministry of Education, Collaborative Innovation Center of Chemical Science and Engineering (Tianjin), Institute of Polymer Chemistry, Nankai University, Tianjin 300071, China.

<sup>b</sup> E-mail: wqzhang@nankai.edu.cn; Fax: 86-22-23503510.

<sup>†</sup> Electronic Supplementary Information (ESI) available: See DOI: 10.1039/x0xx00000x

triblock copolymer core-corona particles increases with the polymerization degree (DP) of the newly introduced A block.

Herein, with the aim to prepare MCBNs, the corona-core nanoparticles of the poly(*N,N*-dimethylacrylamide)-*b*-polystyrene-*b*-poly(4-vinylpyridine) (PDMA-*b*-PS-*b*-P4VP) containing a polystyrene (PS) core and a mixing corona of poly(*N,N*-dimethylacrylamide) (PDMA) and poly(4-vinylpyridine) (P4VP) were initially prepared by seeded RAFT polymerization, and then the corona-forming P4VP block was deposited onto the PS core by dispersing the PDMA-*b*-PS-*b*-P4VP nanoparticles in water, which is a non-solvent for the P4VP block but a solvent for the PDMA block, to convert the PDMA-*b*-PS-*b*-P4VP corona-core nanoparticles into MCBNs.

## 2 Experimental

### 2.1 Materials

The monomers of *N,N*-dimethylacrylamide (DMA, 99.5%, Alfa), styrene (St, >98%, Tianjin Chemical Company), and 4-vinylpyridine (4VP, 96%, Alfa) were distilled under reduced pressure prior to use. The RAFT agent of 4-cyano-4-(dodecylsulfanylthiocarbonyl) sulfanyl pentanoic acid (CDTPA) was synthesized as discussed elsewhere.<sup>45</sup> The initiator of 2,2'-azobis(2-methylpropanitrile) (AIBN, >99%, Tianjin Chemical Company) was purified by recrystallization from ethanol. The internal standard of 1,3,5-trioxane (98%, Alfa) for the <sup>1</sup>H NMR analysis and other reagents were analytic grade and were used as received.

### 2.2 Synthesis of the diblock copolymer seed nanoparticles

The seed nanoparticles of the diblock copolymer of poly(*N,N*-dimethylacrylamide)-*b*-polystyrene trithiocarbonate (PDMA-*b*-PS-TTC, in which TTC represents the RAFT terminal of trithiocarbonate) were prepared by dispersion RAFT polymerization,<sup>41,42</sup> in which (1) the synthesis of the macro-RAFT agent of poly(*N,N*-dimethylacrylamide) trithiocarbonate (PDMA-TTC) by solution RAFT polymerization and (2) the PDMA-TTC macro-RAFT agent mediated dispersion polymerization to afford the diblock copolymer seed nanoparticles was included. The detailed procedures were introduced below.

Into a 100 mL Schlenk flask with a magnetic bar, DMA (10.00 g, 0.101 mol), CDTPA (0.740 g, 1.834 mmol), AIBN (0.030 g, 0.183 mmol), and 1,4-dioxane (40.00 g) were added. The solution was initially degassed with nitrogen at 0 °C, and then the flask content was immersed into a preheated oil bath at 70 °C for 2 h. The polymerization was quenched by rapid cooling upon immersion of the flask in iced water, in which the monomer conversion at 79.0% was determined by <sup>1</sup>H NMR analysis in the presence of the internal standard of 1,3,5-trioxane. The synthesized polymer was precipitated into cold diethyl ether, collected by three precipitation/filtration cycles, and then dried at room temperature under vacuum to afford the PDMA-TTC macro-RAFT agent.

Into a 100 mL Schlenk flask with a magnetic bar, the synthesized PDMA-TTC (1.20 g, 0.255 mol), St (9.27 g, 89.2 mmol), and AIBN (13.9 mg, 0.085 mmol) dissolved in the methanol/water mixture (75/25 by weight, 46.4 g) were added. The oxygen dissolved in the solution was removed by nitrogen purging, and then the polymerization was performed at 70 °C. After 24 h polymerization with the monomer conversion at 99.3%, which was detected by UV-vis analysis at 245 nm as discussed elsewhere,<sup>46</sup> the polymerization was quenched by immersing the flask in iced water. The colloidal dispersion of the *in situ* synthesized PDMA-*b*-PS-TTC nanoparticles was dialyzed against the methanol/water mixture (75/25 by weight) at room temperature for 3 days to remove the residual St monomer and kept at room temperature with the diblock copolymer concentration at 18.0 wt% for the next use. To collect the PDMA-*b*-PS-TTC diblock copolymer for the GPC analysis and <sup>1</sup>H NMR analysis, a given volume of the dispersion of the PDMA-*b*-PS-TTC nanoparticles was separated by centrifugation (12,500 rpm, 15 min), and then dried at room temperature under vacuum to afford the pale yellow powder of the PDMA-*b*-PS-TTC diblock copolymer.

### 2.3 Seeded RAFT polymerization and synthesis of MCBNs of the PDMA-*b*-PS-*b*-P4VP triblock terpolymer

Into a 25 mL Schlenk flask, the alcoholic dispersion of the PDMA-*b*-PS-TTC nanoparticles (2.70 g, containing 0.49 g or 0.012 mmol of PDMA-*b*-PS-TTC and 2.21 g of the 75/25 methanol/water mixture), the initiator of AIBN (0.66 mg, 0.0040 mmol) dissolved in methanol (1.97 g), water (0.66 g), and 4VP (0.50 g, 4.80 mmol) were added. The flask content was degassed with nitrogen at 0 °C to remove oxygen. The polymerization was started by immersing the flask into a preheated oil bath at 70 °C. After a given time, the polymerization was quenched by immersing the flask in iced water.

The monomer conversion in the seeded RAFT polymerization was detected by <sup>1</sup>H NMR analysis, in which a drop of the polymerization solution (about 0.05 mL) was diluted with suitable amount of methanol and a drop of the diluted solution was added into CDCl<sub>3</sub> (0.5 mL) and finally subjected to <sup>1</sup>H NMR analysis to determine the monomer conversion following eq 1, in which *I*<sub>5.45-5.55</sub> is the integral area of the vinyl signals at δ = 5.45-5.55 ppm in the remaining monomer and *I*<sub>8.05-8.57</sub> is the integral area of the pyridyl signals at δ = 8.05-8.57 ppm corresponding to both the 4VP monomer and the P4VP block in the synthesized polymer.

$$\text{conversion (\%)} = \frac{I_{8.05-8.57} - 2I_{5.45-5.55}}{I_{8.05-8.57}} \times 100\% \quad (1)$$

The colloidal dispersion of the *in situ* synthesized PDMA-*b*-PS-*b*-P4VP nanoparticles was dialyzed initially against methanol for 2 days to remove the residual 4VP monomer and then against water at room temperature (20-25 °C) for three days to remove methanol (molecular weight cutoff: 7000 Da) to afford the aqueous dispersion of MCBNs.

To collect the PDMA-*b*-PS-*b*-P4VP triblock terpolymer for the gel permeation chromatography (GPC) analysis and  $^1\text{H}$  NMR analysis, part of the methanol dispersion of the PDMA-*b*-PS-*b*-P4VP triblock terpolymer nanoparticles was precipitated into the mixture of acetone and *n*-hexane (1:1), washed twice with *n*-hexane, and finally dried at room temperature under vacuum to afford the triblock terpolymer in pale yellow.

## 2.4 Characterization

The  $^1\text{H}$  NMR analysis was performed on a Bruker Avance III 400 MHz NMR spectrometer using  $\text{CDCl}_3$  as solvent. To obtain the molecular weight and its distribution or the polydispersity index (PDI,  $\text{PDI} = M_w/M_n$ ) of the synthesized polymers, the GPC analysis was detected using a Viscotek GPC Max Ve2001 solvent/sample module equipped with a DAWN HELEOS 8 light scattering photometer, a ViscoStar viscometer and an Optilab rEX interferometric refractometer from Wyatt Technology Corporation. Samples were passed through three Mz-Gel SD plus 10  $\mu\text{m}$  columns using DMF as eluent at flow rate of 0.8 mL/min at 25°C with narrowly polydispersed polystyrene as calibration standard. TEM observation was performed using a Tecnai G<sup>2</sup> F20 electron microscope at an acceleration of 200 kV. For the PDMA-*b*-PS-*b*-P4VP nanoparticles, two different TEM sampling procedures for the unstained nanoparticles and the nanoparticles stained by phosphotungstic acid (PTA) and  $\text{I}_2$  vapor were adopted, respectively. For the unstained PDMA-*b*-PS-*b*-P4VP nano-objects, a small drop of the diluted colloidal dispersion was dripped onto a piece of copper grid, dried at room temperature till the solvent was evaporated, and finally checked by TEM; for the PDMA-*b*-PS-*b*-P4VP nano-objects jointly stained by PTA and  $\text{I}_2$  vapor, into the diluted dispersion of the triblock terpolymer nano-objects (1 mL), a drop of 1.5 wt% PTA aqueous solution ( $\sim 0.01$  mL) was added, kept at room temperature for 2 min, and then a small drop of the colloids was dripped onto a piece of copper grid, dried at room temperature, and then stained by  $\text{I}_2$  vapor at 50 °C for 30 min under reduced pressure, and finally observed by TEM. DSC analysis was carried out on a NETZSCH differential scanning calorimeter under nitrogen atmosphere, in which the sample was heated to 200 °C at the heating rate of 10 °C/min, cooled to -20 °C in 5 min, and then heated to 200 °C at the heating rate of 10 °C/min.

## 3 Result and discussion

### 3.1 Synthesis of the seed nanoparticles of the PDMA-*b*-PS-TTC diblock copolymer

The seed nanoparticles of the PDMA-*b*-PS-TTC diblock copolymer was synthesized by the PDMA-TTC macro-RAFT agent mediated dispersion polymerization of styrene in the 75/25 methanol/water mixture.<sup>41</sup> This dispersion RAFT polymerization is used to prepare the seed nanoparticles of the PDMA-*b*-PS-TTC diblock copolymer, since it can afford the *in situ* synthesis of the concentrated block copolymer nanoparticles as discussed elsewhere.<sup>47-51</sup>

To prepare the PDMA-*b*-PS-TTC seed nanoparticles, the PDMA-TTC macro-RAFT agent was initially synthesized by solution RAFT polymerization under  $[\text{DMA}]_0:[\text{CDTPA}]_0:[\text{AIBN}]_0 = 550:10:1$ . The RAFT polymerization of DMA was quenched at 79.0% monomer conversion to ensure the narrowly dispersed molecular weight of the synthesized PDMA-TTC macro-RAFT agent. The theoretical number-average molecular weight,  $M_{n,\text{th}}$  of PDMA-TTC is 4.71 kg/mol, corresponding to the polymerization degree (DP) at 43, in which  $M_{n,\text{th}}$  is calculated following eq 2 as discussed elsewhere.<sup>14</sup> The DMF based GPC analysis gives the polymer molecular weight  $M_{n,\text{GPC}} = 4.90$  kg/mol, which is very close to  $M_{n,\text{th}}$  and the molecular weight distribution is narrow as indicated by the low PDI value at 1.13 (Figure 1). The  $^1\text{H}$  NMR spectrum of PDMA-TTC is shown in Figure 2A. Based on the characteristic chemical shift of the RAFT terminal at  $\delta = 0.88$  ppm and the PDMA<sub>43</sub>-TTC backbone at  $\delta = 2.90$  ppm, the molecular weight of PDMA<sub>43</sub>-TTC,  $M_{n,\text{NMR}}$  at 5.06 kg/mol was calculated, which is very close to  $M_{n,\text{th}}$ . In the subsequent discussion, the synthesized PDMA-TTC is labelled as PDMA<sub>43</sub>-TTC, in which the DP of 43 is determined by the theoretical number-average molecular weight  $M_{n,\text{th}}$ .

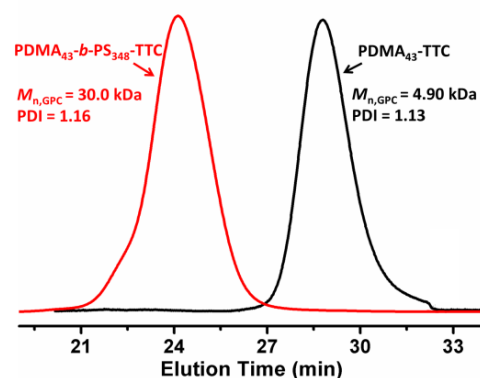


Fig 1. The GPC traces of PDMA<sub>43</sub>-TTC and PDMA<sub>43</sub>-*b*-PS<sub>348</sub>-TTC.

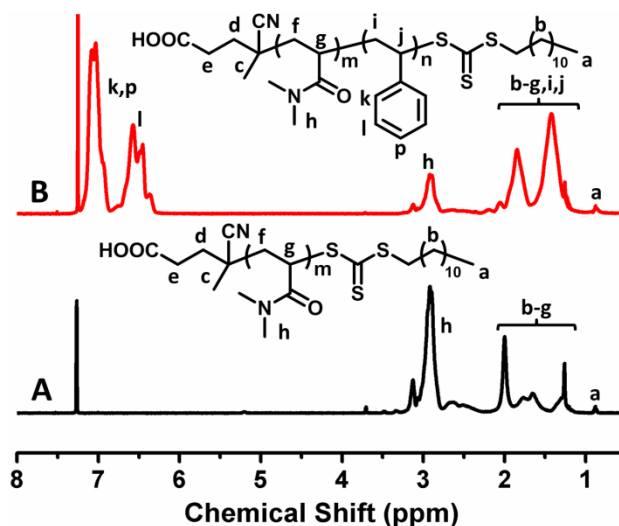
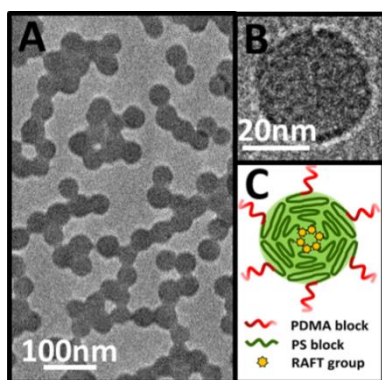


Fig 2.  $^1\text{H}$  NMR spectra of PDMA<sub>43</sub>-TTC (A) and PDMA<sub>43</sub>-*b*-PS<sub>348</sub>-TTC (B).

$$M_{n,th} = \frac{[monomer]_0 \times M_{monomer}}{[RAFT]_0} \times conversion + M_{RAFT} \quad (2)$$



**Fig 3.** The TEM images of the PDMA<sub>43</sub>-*b*-PS<sub>348</sub>-TTC seed nanoparticles (A, B) and the schematic structure (C) of the PDMA<sub>43</sub>-*b*-PS<sub>348</sub>-TTC seed nanoparticles dispersed in the alcoholic solvent.

The PDMA-TTC macro-RAFT agent mediated dispersion polymerization of St in the 75/25 methanol/water mixture under  $[St]_0:[PDMA_{43}\text{-TTC}]_0:[AIBN]_0 = 1050:3:1$  affords the *in situ* synthesis of the seed nanoparticles of the PDMA-*b*-PS-TTC diblock copolymer, which is indicated by the polymerization mixture becoming turbid at 2.5 h. After 24 h polymerization, the polymerization was quenched, and 99.3% monomer conversion was obtained, and the *in situ* synthesis of the PDMA-*b*-PS-TTC nanoparticles was achieved. After removal of the residual St monomer by dialysis against the alcoholic solvent, the diblock copolymer nanoparticles were characterized by TEM. As shown in Figures 3A and 3B, uniform seed nanoparticles of the PDMA-*b*-PS-TTC diblock copolymer with the average size at 36 nm are formed. Since the PDMA block is soluble and the PS block is insoluble in the alcoholic solvent, the PDMA<sub>43</sub>-*b*-PS<sub>348</sub>-TTC nanoparticles are expected to have corona-core structure as shown in Figure 3C, in which the solvophilic PDMA block forms the corona and the solvophobic PS block forms the core, and the Z-group RAFT terminal at the end of the PS block should be located in the inner PS core of the corona-core nanoparticles. Based on the DP of the PS block at 348, which will be discussed subsequently, the maximum length  $L_{max}$  of the extended chain of the PS<sub>348</sub> block, 44 nm, is calculated, which is much larger than the radius, 18 nm, of the PS core, and therefore the compacted conformation of the PS chains in the core of the seed nanoparticles as shown in Figure 3C is expected. Based on eq 3,<sup>52</sup> in which  $D$  represents the

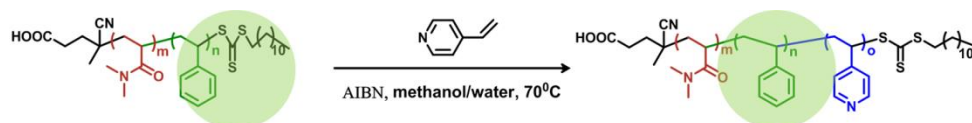
average diameter by TEM,  $d_p$  represents the polymer density approximately at 1.0 g/cm<sup>3</sup>,  $N_A$  represents the Avogadro's number, and  $M_{n,PS}$  represents the molecular weight of the PS block, respectively, the aggregation number  $N_{agg}$  of the PDMA-*b*-PS-TTC nanoparticles, 406, is approximately calculated, and therefore the number-density of the PDMA chains tethered on the PS core, 0.100 nm<sup>-2</sup>, is obtained.

$$N_{agg} = \frac{\pi D^3 d_p N_A}{6 M_{n,PS}} \quad (3)$$

The polymer constructing the PDMA-*b*-PS-TTC nanoparticles was characterized by GPC analysis and <sup>1</sup>H NMR analysis (Figure 1 and 2). Figure 1 shows the GPC trace of the synthesized PDMA-*b*-PS-TTC diblock copolymer, from which the molecular weight  $M_{n,GPC}$  of PDMA-*b*-PS-TTC at 30.0 kg/mol with PDI = 1.16 is obtained. Compared with the theoretical molecular weight  $M_{n,th}$  at 40.9 kg/mol, which is calculated following eq 2, the  $M_{n,GPC}$  of PDMA-*b*-PS-TTC is smaller, and the reason is possibly due to the polystyrene standard employed in the GPC analysis. The <sup>1</sup>H NMR spectrum of the PDMA-*b*-PS-TTC diblock copolymer is shown in Figure 2B. Based on the characteristic chemical shift of the PDMA block at  $\delta = 2.90$  ppm and that in the phenyl groups of the PS block at  $\delta = 7.22\text{-}6.26$  ppm, the  $M_{n,NMR}$  at 44.1 kg/mol of the PDMA-*b*-PS-TTC diblock copolymer is calculated. Clearly,  $M_{n,NMR}$  of the PDMA-*b*-PS-TTC diblock copolymer is close to  $M_{n,th}$ , and therefore this diblock copolymer is labelled as PDMA<sub>43</sub>-*b*-PS<sub>348</sub>-TTC, in which the DP of the PS block is determined by  $M_{n,th}$  in the subsequent discussion.

### 3.2 Seeded RAFT polymerization and synthesis of MCBNs of the PDMA-*b*-PS-*b*-P4VP triblock terpolymer

The seeded RAFT polymerization was performed under  $[4VP]_0:[PDMA_{43}\text{-}b\text{-PS}_{348}\text{-TTC}]_0:[AIBN]_0 = 1200:3:1$  in the 75/25 methanol/water mixture. Different from the general RAFT polymerization employing a soluble RAFT agent,<sup>47-51,53-56</sup> the PDMA<sub>43</sub>-*b*-PS<sub>348</sub>-TTC nanoparticles are used as seed in the seeded RAFT polymerization. With the proceeding of the seeded RAFT polymerization, the third P4VP block, which is soluble in the polymerization medium of the alcoholic solvent, is introduced into the end of the PS block and the introduced P4VP block extends with the increasing monomer conversion, and the PDMA<sub>43</sub>-*b*-PS<sub>348</sub>-TTC seed nanoparticles are converted into the PDMA<sub>43</sub>-*b*-PS<sub>348</sub>-*b*-P4VP triblock terpolymer corona-core nanoparticles containing a PS core and a mixed core of the PDMA and P4VP blocks as shown in Scheme 2.



**Scheme 2.** Seeded RAFT polymerization to synthesize the corona-core nanoparticles of PDMA-*b*-PS-*b*-P4VP containing a mixed corona.

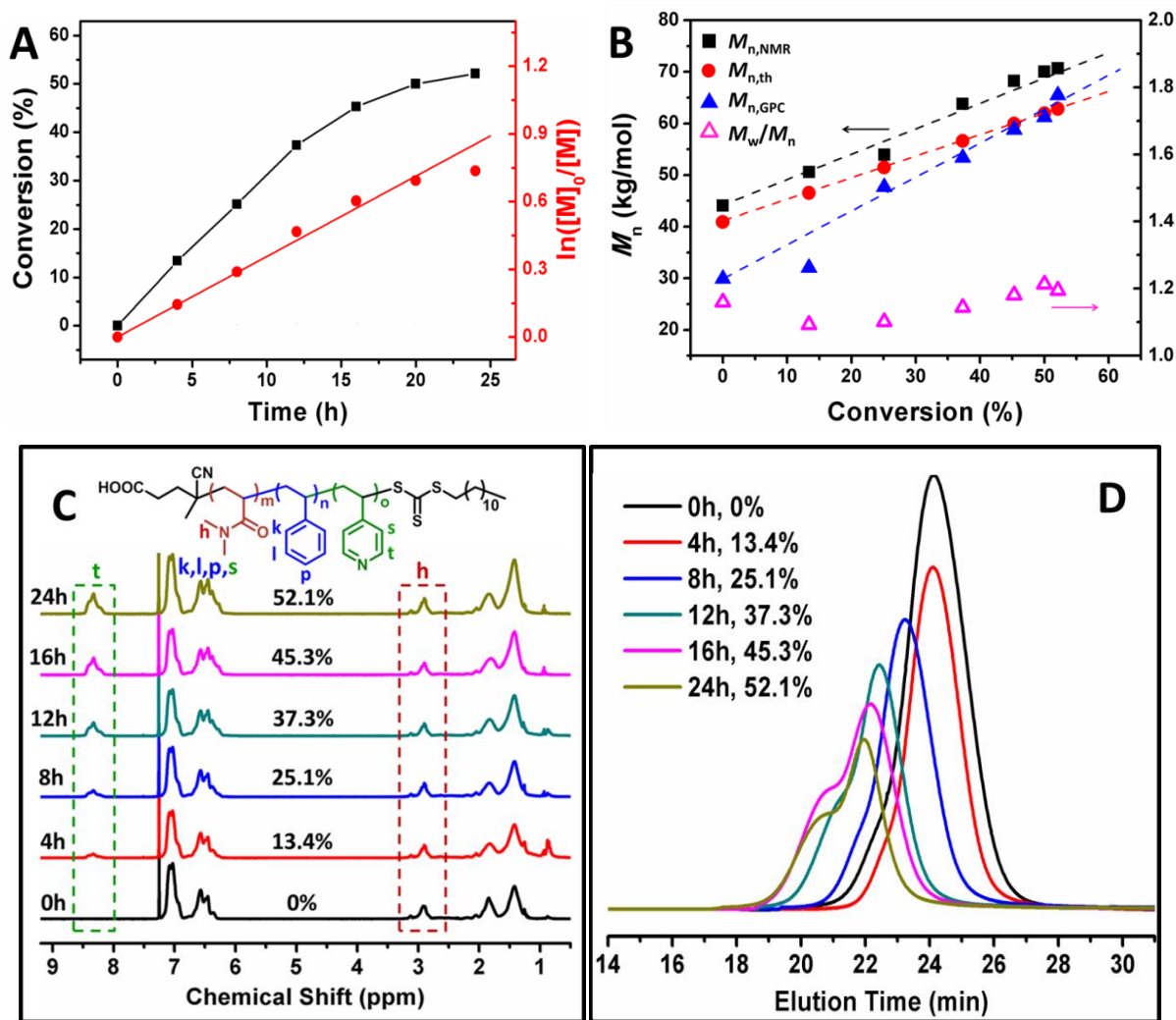


**Fig 4.** The monomer conversion-time plot and the  $\ln([M]_0/[M])$ -time plot (A) for the seeded RAFT polymerization, the molecular weight and PDI (B), the  $^1H$  NMR spectra (C), and the GPC traces (D) of the synthesized PDMA-*b*-PS-*b*-P4VP triblock terpolymers. Polymerization conditions: 4VP (1.00 g, 9.52 mmol), the methanol/water mixture (9.63 g, 75/25 by weight),  $[4VP]_0/[PDMA\text{-}b\text{-}PS\text{-}TTC]_0/[AIBN]_0 = 1200/3/1$ , 70 °C.

The polymerization kinetics of the seeded RAFT polymerization is summarized in Figure 4A. The monomer conversion increases with the polymerization time and finally it reached 50.0% in 20 h. The further increase in the polymerization time just leads to a very slight increase in the monomer conversion. This is partly due to the diluted 4VP monomer concentration at ~4% in the later stage of the seeded RAFT polymerization. From the linear  $\ln([M]_0/[M])$ -time plot, the pseudo-first-order kinetics of the seeded RAFT polymerization just like a general homogeneous RAFT polymerization is concluded. The PDMA<sub>43</sub>-*b*-PS<sub>348</sub>-*b*-P4VP triblock terpolymers synthesized at different polymerization times are characterized by  $^1H$  NMR analysis and GPC analysis, and the results are summarized in Figure 4B. From the  $^1H$  NMR spectra shown in Figure 4C, the increasing signal at  $\delta = 8.05$ - $8.57$  ppm corresponding to the pyridine group in the P4VP block as indicated out by the green rectangle with the polymerization time is detected, indicating the chain extension of the P4VP block in the PDMA<sub>43</sub>-*b*-PS<sub>348</sub>-*b*-P4VP triblock

terpolymer during the RAFT polymerization. The molecular weight  $M_{n,NMR}$  of the triblock terpolymer is calculated by comparing the area ratio of the characteristic chemical shift of the pyridine ring in the P4VP block to that of the benzene ring following eq 4, and the linear increase of  $M_{n,NMR}$  with the monomer conversion as summarized in Figure 4B is found. From the GPC traces shown in Figure 4D, the molecular weight,  $M_{n,GPC}$ , of the PDMA<sub>43</sub>-*b*-PS<sub>348</sub>-*b*-P4VP triblock terpolymers and the PDI values are obtained. As summarized in Figure 4B,  $M_{n,GPC}$  of the PDMA<sub>43</sub>-*b*-PS<sub>348</sub>-*b*-P4VP triblock terpolymers linearly increases with the monomer conversion, and the PDI values locating at 1.1-1.3 slightly increase with the monomer conversion. The increasing PDI values at the case of the high monomer conversion is possibly ascribed to the bimolecular radical termination in the seeded RAFT polymerization, which is indicated out by the slight shoulder at the high molecular weight side in the GPC traces. Furthermore, it is found that the  $M_{n,NMR}$  and  $M_{n,th}$  of the PDMA<sub>43</sub>-*b*-PS<sub>348</sub>-*b*-P4VP triblock terpolymer are close to each other, whereas the  $M_{n,GPC}$  is a

little smaller. The reason is possibly ascribed to the polystyrene standard used in the GPC analysis. All together, the good control both on the polymer molecular weight and on the molecular weight distribution in the seeded RAFT polymerization is achieved.

$$M_{n,NMR} = \frac{5I_{8.05-8.57}}{2(I_{6.26-7.22} - I_{8.05-8.57})} \times DP_{PS} \times M_{4VP} + M_{n,PDMA-b-PS-TTC} \quad (4)$$

The PDMA<sub>43</sub>-*b*-PS<sub>348</sub>-*b*-P4VP triblock terpolymers as well as the reference polymers of PDMA<sub>43</sub>-TTC, PS<sub>250</sub>-TTC, P4VP<sub>95</sub>-TTC and the PDMA<sub>43</sub>-*b*-PS<sub>348</sub>-TTC diblock copolymer were further characterized by DSC analysis. As shown in Figure 5, the glass transition temperature ( $T_g$ ) of the reference homopolymer of PDMA<sub>43</sub>-TTC, PS<sub>250</sub>-TTC and P4VP<sub>95</sub>-TTC is 105.7, 96.4 and 140.1 °C, respectively. As to the PDMA<sub>43</sub>-*b*-PS<sub>348</sub>-TTC diblock copolymer, the single  $T_g$  at 105.5 °C is detected, and the reason is possibly due to the two  $T_g$  values of the PS and PDMA blocks being very similar to each other or the PS and PDMA blocks being somewhat compatible. In the DSC thermograms of the PDMA<sub>43</sub>-*b*-PS<sub>348</sub>-*b*-P4VP<sub>208</sub> triblock terpolymer, two separate  $T_g$  values at 104.7 °C corresponding to the PS and/or PDMA blocks and at 146.6 °C corresponding

to the P4VP block are clearly discerned, suggesting the third P4VP block is immiscible with the PS block,<sup>14</sup> which affords the potential of the P4VP block depositing onto the PS core to form discrete P4VP microphases on the PS core to form MCBNs.

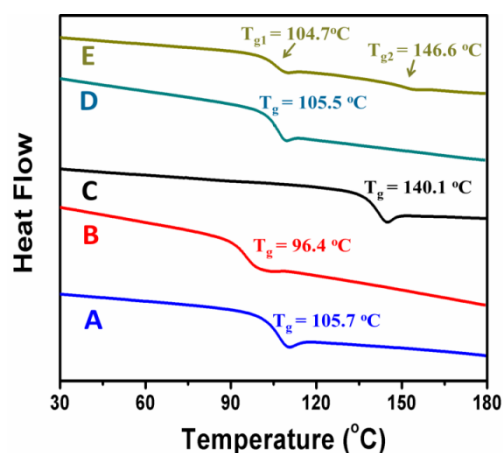


**Fig 5.** DSC thermograms of PDMA<sub>43</sub>-TTC (A), PS<sub>250</sub>-TTC (B), P4VP<sub>95</sub>-TTC (C), PDMA<sub>43</sub>-*b*-PS<sub>348</sub>-TTC (D), and PDMA<sub>43</sub>-*b*-PS<sub>348</sub>-*b*-P4VP<sub>208</sub> (E).

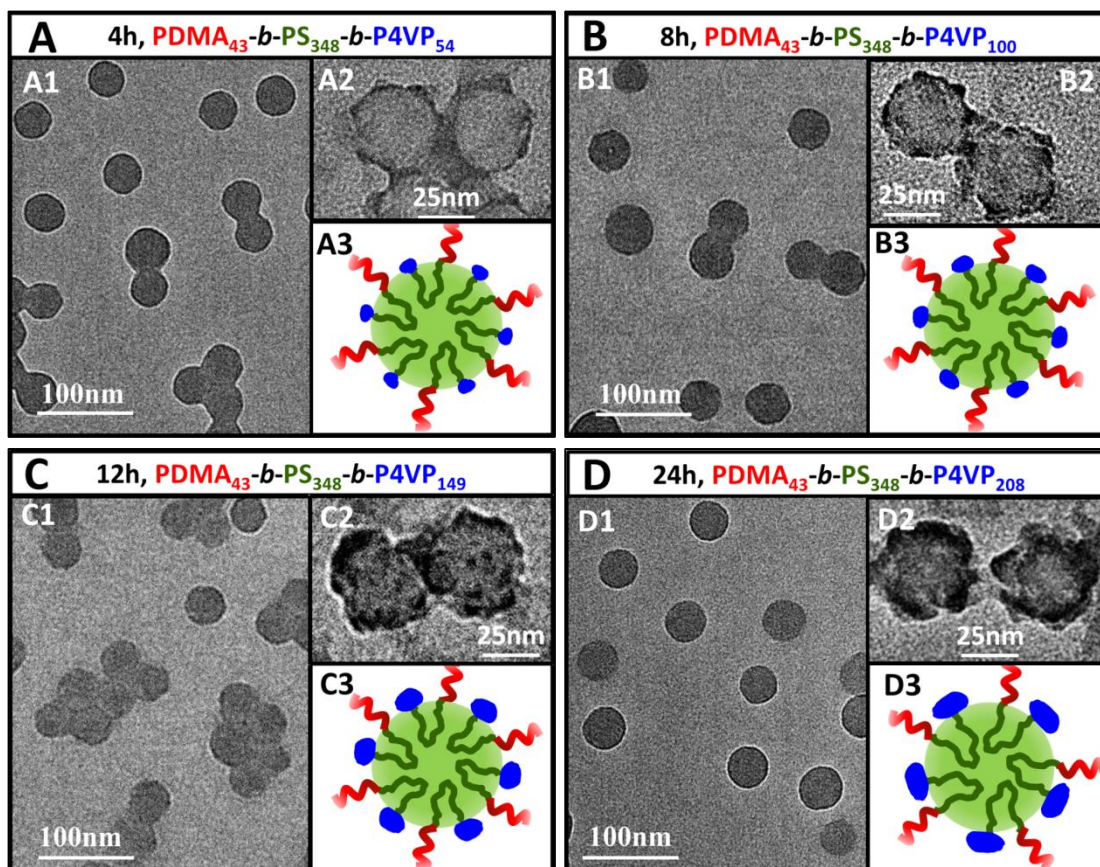


**Fig 6.** TEM images of the unstained MCBNs of PDMA<sub>43</sub>-*b*-PS<sub>348</sub>-*b*-P4VP (A1-D4) and the MCBNs stained jointly by PTA and I<sub>2</sub> vapor (A2-D2), and the schematic structure of MCBNs (A3-D3) prepared at the polymerization time of 4 h (A), 8 h (B), 12 h (C), and 24 h (D).

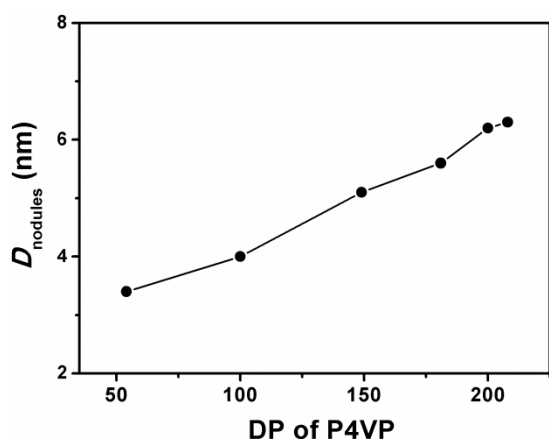


**Fig 7.** The average diameter  $D_{\text{nodules}}$  of the P4VP microphases on the MCBNs of PDMA<sub>43</sub>-*b*-PS<sub>348</sub>-*b*-P4VP with the different DP of the P4VP block.

The seeded RAFT polymerization affords the *in situ* synthesis of the PDMA-*b*-PS-*b*-P4VP corona-core nanoparticles containing a mixed corona of the PDMA and P4VP blocks in the alcoholic solvent. To convert these corona-core nanoparticles into MCBNs, these corona-core nanoparticles dispersed in the alcoholic solvent were transferred into water by dialysis against water. In water, the core of the PS block is frozen at room temperature since the PS block with a relatively high  $T_g$  at 96.4 °C is insoluble in water. Whereas for the corona-forming blocks of PDMA and P4VP, the P4VP block becomes insoluble in neutral water and deposits onto the PS core to form the discrete microphases onto the PS core to form MCBNs, and the PDMA block is soluble in water and keeps the MCBNs of the PDMA-*b*-PS-*b*-P4VP triblock terpolymer suspending in water, respectively. Figure 6 shows the TEM images of the MCBNs nanoparticles of the PDMA-*b*-PS-*b*-P4VP triblock terpolymers with different DP of the P4VP block before and after being stained with PTA and I<sub>2</sub> vapor (Figures 6A1-6D1 and Figures 6A2-6D2). Note: PTA and I<sub>2</sub> vapor can selectively stain the P4VP microphases on the PDMA-*b*-PS-*b*-P4VP MCBNs nanoparticles as discussed elsewhere,<sup>36</sup> and therefore helps to discern the P4VP microphases on MCBNs. As shown by the TEM images in Figures 6A1-6D1, nanospheres with the average size at 38-41 nm are observed in the four cases of the DP of the P4VP block. The results indicate that the DP of the P4VP block have no or very slight influence on the size of the PDMA-*b*-PS-*b*-P4VP nanoparticles. Besides, the P4VP microphases cannot be discerned, and the reason is possibly due to the small size of the P4VP microphases and the similar electron density of the P4VP and PS microphases. After the PDMA-*b*-PS-*b*-P4VP nanoparticles being stained by PTA and I<sub>2</sub> vapor, the P4VP microphase in the PDMA-*b*-PS-*b*-P4VP nanoparticles as indicated by the dark domain in the TEM images (Figures 6A2-6D2) can be clearly discerned. Note: the light gray region corresponds to the PS core, the dark domain corresponds to the stained P4VP microphases deposited on the PS core, and the solvophilic PDMA corona is invisible in the TEM images. These TEM images confirm the formation of the MCBNs of the PDMA<sub>43</sub>-*b*-PS<sub>348</sub>-*b*-P4VP triblock terpolymer,

which contain a PS core, the discrete P4VP microphases (nodules) on the PS core, and a solvated PDMA corona as schematically shown in Figures 6A3-D3. By carefully checking the P4VP microphases on the PS core, it is also found that the average diameter or extension of the P4VP nodules ( $D_{\text{nodules}}$ ) increases from 3 to 6 nm when the DP of the P4VP block increases from 54 to 208 as shown in Figure 7, although just an approximate size estimation is made.

## 4 Conclusions

Seeded RAFT polymerization is proposed to prepare MCBNs of the PDMA<sub>43</sub>-*b*-PS<sub>348</sub>-*b*-P4VP triblock terpolymer, which contain a PS core, the dispersed P4VP microphases on the PS core, and a solvated PDMA corona. Following this seeded RAFT polymerization, the diblock copolymer corona-core nanoparticles of PDMA<sub>43</sub>-*b*-PS<sub>348</sub>-TTC containing a PDMA corona and a PS core are prepared through the PDMA<sub>43</sub>-TTC macro-RAFT agent mediated dispersion polymerization, and then the corona-core nanoparticles of PDMA<sub>43</sub>-*b*-PS<sub>348</sub>-TTC are used as seed in seeded RAFT polymerization, onto which the third P4VP block is introduced, and the triblock terpolymer corona-core nanoparticles of PDMA<sub>43</sub>-*b*-PS<sub>348</sub>-*b*-P4VP containing a PS core and a mixed corona of P4VP and PDMA are prepared. The seeded RAFT polymerization undergoes a pseudo-first-order kinetics, and the molecular weight of the PDMA<sub>43</sub>-*b*-PS<sub>348</sub>-*b*-P4VP triblock terpolymer with relatively low PDI increases linearly with the monomer conversion. When the corona-core nanoparticles of PDMA<sub>43</sub>-*b*-PS<sub>348</sub>-*b*-P4VP are dispersed in water, the P4VP chains, which are segregated by the neighbouring PDMA chains, deposit onto the PS core to form discrete P4VP microphases on the PS core and the corona-core nanoparticles convert into MCBNs containing a PS core, the discrete P4VP microphases on the PS core, and a solvated PDMA corona. It is found that the size of the P4VP microphases on the PS core increases with the DP of the P4VP block. Our strategy of the seeded RAFT polymerization is believed to be a valid method to prepare MCBNs of ABC triblock terpolymer.

## Acknowledgements

The financial support by National Science Foundation of China (No 21274066 and 21474054), and PCSIRT (IRT1257) is gratefully acknowledged.

## Notes and references

1. A. O. Moughton, M. A. Hillmyer and T. P. Lodge, *Macromolecules*, 2012, **45**, 2-19.
2. J.-F. Lutz and A. Laschewsky, *Macromol. Chem. Phys.*, 2005, **206**, 813-817.
3. E. Amado and J. Kressler, *Soft Matter*, 2011, **7**, 7144.
4. A. H. Gröschel, A. Walther, T. I. Löbbling, F. H. Schacher, H. Schmalz and A. H. E. Müller, *Nature*, 2013, **503**, 247-251.
5. B. Fang, A. Walther, A. Wolf, Y. Xu, J. Yuan and A. H. E. Müller *Angew. Chem. Int. Ed.*, 2009, **48**, 2877-2880.

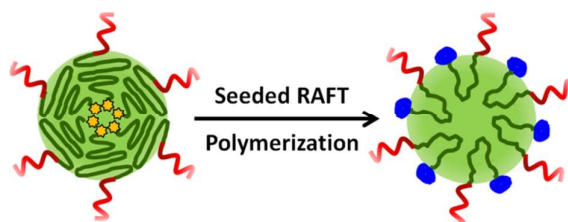


- 6 A. H. Gröschel, A. Walther, T. I. Löbling, J. Schmelz, A. Hanisch, H. Schmalz and A. H. E. Müller, *J. Am. Chem. Soc.*, 2012, **134**, 13850-13860.
- 7 R. R. Taribagil, M. A. Hillmyer and T. P. Lodge, *Macromolecules*, 2010, **43**, 5396-5404.
- 8 G. Sun, H. Cui, L. Y. Lin, N. S. Lee, C. Yang, W. L. Neumann, J. N. Freskos, J. J. Shieh, R. B. Dorshow and K. L. Wooley, *J. Am. Chem. Soc.*, 2011, **133**, 8534-8543.
- 9 H. Cui, Z. Chen, S. Zhong, K. L. Wooley and D. J. Pochan, *Science*, 2007, **317**, 647-650.
- 10 J.-N. Marsat, M. Heydenreich, E. Kleinpeter, H. V. Berlepsch, C. Böttcher and A. Laschewsky, *Macromolecules*, 2011, **44**, 2092-2105.
- 11 S. Kubowicz, J.-F. Baussard, J.-F. Lutz, A. F. Thünemann, H. V. Berlepsch and A. Laschewsky, *Angew. Chem. Int. Ed.*, 2005, **44**, 5262-5265.
- 12 Y. Gao, X. Li, L. Hong and G. Liu, *Macromolecules*, 2012, **45**, 1321-1330.
- 13 J. Dupont and G. Liu, *Soft Matter*, 2010, **6**, 3654-3661.
- 14 F. Huo, S. Li, Q. Li, Y. Qu and W. Zhang, *Macromolecules*, 2014, **47**, 2340-2349.
- 15 F. Schacher, A. Walther, M. Ruppel, M. Drechsler and A. H. E. Müller, *Macromolecules*, 2009, **42**, 3540-3548.
- 16 Z. Li, E. Kesselman, Y. Talmon, M. A. Hillmyer and T. P. Lodge, *Science*, 2004, **306**, 97-101.
- 17 N. Saito, C. Liu, T. P. Lodge and M. A. Hillmyer, *Macromolecules*, 2008, **41**, 8815-8822.
- 18 A. Hanisch, A. H. Gröschel, M. Förtsch, M. Drechsler, H. Jinnai, T. M. Ruhland, F. H. Schacher and A. H. E. Müller, *ACS Nano*, 2013, **7**, 4030-4041.
- 19 J.-F. Gohy, C. Ott, S. Hoepfener and U. S. Schubert, *Chem. Commun.*, 2009, 6038-6040.
- 20 J. Zhu, S. Zhang, K. Zhang, X. Wang, J. W. Mays, K. L. Wooley and D. J. Pochan, *Nature Commun.*, 2013, **4**, 1-7.
- 21 D. J. Pochan, J. Zhu, K. Zhang, K. L. Wooley, C. Miesch and T. Emrick, *Soft Matter*, 2011, **7**, 2500-2506.
- 22 Z. Li, M. A. Hillmyer and T. P. Lodge, *Macromolecules*, 2006, **39**, 765-771.
- 23 R. Zheng, G. Liu and X. Yan, *J. Am. Chem. Soc.*, 2005, **127**, 15358-15359.
- 24 G. Srinivas and J. W. Pitera, *Nano Lett.*, 2008, **8**, 611-618.
- 25 X. Yan, G. Liu and J. Hu, *Macromolecules*, 2006, **39**, 1906-1912.
- 26 F. Schacher, E. Betthausen, A. Walther, H. Schmalz, D. V. Pergushov and A. H. E. Müller, *ACS Nano*, 2009, **3**, 2095-2102.
- 27 J. Zhu, S. Zhang, F. Zhang, K. L. Wooley and D. J. Pochan, *Adv. Funct. Mater.*, 2013, **23**, 1767-1773.
- 28 J. Zhu and R. C. Hayward, *Macromolecules*, 2008, **41**, 7794-7797.
- 29 J.-F. Gohy, N. Lefèvre, C. D'Haese, S. Hoepfener, U. S. Schubert, G. Kostov and B. Améduri, *Polym. Chem.*, 2011, **2**, 328-332.
- 30 D. A. Christian, A. Tian, W. G. Ellenbroek, I. Levental, K. Rajagopal, P. A. Janmey, A. J. Liu, T. Baumgart and D. E. Discher, *Nature Mater.*, 2009, **8**, 843-849.
- 31 E. W. Price, Y. Guo, C.-W. Wang and M. G. Moffitt, *Langmuir*, 2009, **25**, 6398-6406.
- 32 X. Liu, H. Gao, F. Huang, X. Pei, Y. An, Z. Zhang and L. Shi, *Polymer*, 2013, **54**, 3633-3640.
- 33 L. Cheng, X. Lin, F. Wang, B. Liu, J. Zhou, J. Li and W. Li, *Macromolecules*, 2013, **46**, 8644-8648.
- 34 X. He, Q. Li, P. Shi, Y. Cui, S. Li and W. Zhang, *Polym. Chem.*, 2014, **5**, 7090-7099.
- 35 S. Li, X. He, Q. Li, P. Shi and W. Zhang, *ACS Macro Lett.*, 2014, **3**, 916-921.
- 36 P. Shi, Q. Li, X. He, S. Li, P. Sun and W. Zhang, *Macromolecules*, 2014, **47**, 7442-7452.
- 37 Q. Li, X. He, Y. Cui, P. Shi, S. Li and W. Zhang, *Polym. Chem.*, 2015, **6**, 70-78.
- 38 J.-F. Gohy, E. Khouzakoun, N. Willet, S. K. Varshney and R. Jérôme, *Macromol. Rapid Commun.*, 2004, **25**, 1536-1539.
- 39 P. Chambon, A. Blanazs, G. Battaglia and S. P. Armes, *Macromolecules*, 2012, **45**, 5081-5090.
- 40 X. Shen, F. Huo, H. Kang, S. Zhang, J. Li and W. Zhang, *Polym. Chem.*, 2015, **6**, 3407-3414.
- 41 M. Dan, F. Huo, X. Xiao, Y. Su and W. Zhang, *Macromolecules*, 2014, **47**, 1360-1370.
- 42 H. Kang, Y. Su, X. He, S. Zhang, J. Li and W. Zhang, *J. Polym. Sci., Part A: Polym. Chem.*, 2015, **53**, 1777-1784.
- 43 F. Huo, C. Gao, M. Dan, X. Xiao, Y. Su and W. Zhang, *Polym. Chem.*, 2014, **5**, 2736-2746.
- 44 A. Li, J. Ma, G. Sun, Z. Li, S. Cho, C. Clark and K. L. Wooley, *J. Polym. Sci., Part A: Polym. Chem.*, 2012, **50**, 1681-1688.
- 45 G. Moad, Y. K. Chong, A. Postma, E. Rizzardo and S. H. Thang, *Polymer*, 2005, **46**, 8458-8468.
- 46 C. Gao, Q. Li, Y. Cui, F. Huo, S. Li, Y. Su, and W. Zhang, *J. Polym. Sci. Part A: Polym. Chem.*, 2014, **52**, 2155-2165.
- 47 S. Sugihara, A. Blanazs, S. P. Armes, A. J. Ryan and A. L. Lewis, *J. Am. Chem. Soc.*, 2011, **133**, 15707-15713.
- 48 Y. Pei and A. B. Lowe, *Polym. Chem.*, 2014, **5**, 2342-2351.
- 49 J.-T. Sun, C.-Y. Hong and C.-Y. Pan, *Soft Matter*, 2012, **8**, 7753-7767.
- 50 B. Charleux, G. Delaittre, J. Rieger and F. D'Agosto, *Macromolecules*, 2012, **45**, 6753-6765.
- 51 E. R. Jones, M. Semsarilar, A. Blanazs and S. P. Armes, *Macromolecules*, 2012, **45**, 5091-5098.
- 52 C. Zhou, M. A. Hillmyer and T. P. Lodge, *Macromolecules*, 2011, **44**, 1635-1641.
- 53 W. Shen, Y. Chang, G. Liu, H. Wang, A. Cao and Z. An, *Macromolecules*, 2011, **44**, 2524-2530.
- 54 X. Zhang, S. Boissé, C. Bui, P.-A. Albouy, A. Brûlet, M.-H. Li, J. Rieger and B. Charleux, *Soft Matter*, 2012, **8**, 1130-1141.
- 55 Y. Pei, N. C. Dharsana, J. A. van Hensbergen, R. P. Burford, P. J. Roth and A. B. Lowe, *Soft Matter*, 2014, **10**, 5787-5796.
- 56 M. Semsarilar, V. Ladmiraal, A. Blanazs and S. P. Armes, *Langmuir*, 2012, **28**, 914-922.

**For Table of Contents use only****Synthesis of multicompartment nanoparticles of triblock terpolymer by seeded RAFT polymerization**

Xin He, Yaqing Qu, Chengqiang Gao and Wangqing Zhang\*

Key Laboratory of Functional Polymer Materials of the Ministry of Education, Collaborative Innovation Center of Chemical Science and Engineering (Tianjin), Institute of Polymer Chemistry, Nankai University, Tianjin 300071, China.



Seeded RAFT polymerization based on AB diblock copolymer nanoparticles is performed, and multicompartment nanoparticles of ABC triblock terpolymer is prepared.